land

MDPI

Article

Exploring Ecological Quality and Its Driving Factors in Diqing Prefecture, China, Based on Annual Remote Sensing Ecological Index and Multi-Source Data

Chen Wang [1,2,3,4], Qianqian Sheng [1,2,3,4,*] and Zunling Zhu [1,2,3,4,5,*]

1 College of Landscape Architecture, Nanjing Forestry University, Nanjing 210037, China; wangchen1999@njfu.edu.cn
2 The Center of Southern Modern Forestry Cooperative Innovation, Nanjing Forestry University, Nanjing 210037, China
3 Research Center for Digital Innovation Design, Nanjing Forestry University, Nanjing 210037, China
4 Jin Pu Research Institute, Nanjing Forestry University, Nanjing 210037, China
5 College of Art and Design, Nanjing Forestry University, Nanjing 210037, China
* Correspondence: qqs@njfu.edu.cn (Q.S.); zhuzunling@njfu.edn.cn (Z.Z.)

Abstract: The interaction between the natural environmental and socioeconomic factors is crucial for assessing the dynamics of plateau ecosystems. Therefore, the remote sensing ecological index (RSEI) and CatBoost-SHAP model were employed to investigate changes in the ecological quality and their driving factors in the Diqing Tibetan Autonomous Prefecture, China, from 2001 to 2021. The results showed an increase from 0.44 in 2001 to 0.71 in 2021 in the average RSEI for the Diqing Prefecture, indicating an overall upward trend in the ecological quality. Spatial analysis shows the percentage of the area covered by different levels of RSEI and their temporal changes. The results revealed that "good" ecological quality accounted for the largest proportion of the study area, at 42.77%, followed by "moderate" at 21.93%, and "excellent" at 16.62%. "Fair" quality areas accounted for 16.11% and "poor" quality areas only 2.57%. The study of ecological and socioeconomic drivers based on the CatBoost-SHAP framework also indicated that natural climate factors have a greater impact on ecological quality than socioeconomic factors; however, this effect differed significantly with altitude. The findings suggest that, in addition to strengthening climate monitoring, further advancements in ecological engineering are required to ensure the sustainable development of the ecosystem and the continuous improvement of the environmental quality in the Diqing Prefecture.

Keywords: ecological quality; remote sensing ecological index (RSEI); CatBoost-SHAP framework; change analysis; driver analysis

check for updates

Citation: Wang, C.; Sheng, Q.; Zhu, Z. Exploring Ecological Quality and Its Driving Factors in Diqing Prefecture, China, Based on Annual Remote Sensing Ecological Index and Multi-Source Data. *Land* **2024**, *13*, 1499. https://doi.org/10.3390/land13091499

Academic Editor: Todd Robinson

Received: 29 August 2024
Revised: 12 September 2024
Accepted: 13 September 2024
Published: 15 September 2024

Copyright: © 2024 by the authors. Licensee MDPI, Basel, Switzerland. This article is an open access article distributed under the terms and conditions of the Creative Commons Attribution (CC BY) license (https://creativecommons.org/licenses/by/4.0/).

1. Introduction

At the beginning of the 21st century, global environmental change has emerged as a major challenge for society. The significant increase in greenhouse gas emissions owing to anthropogenic activities has had complex and diverse impacts on ecosystem health and sustainability, and environmental issues such as biodiversity loss [1–3], water scarcity [4,5], and vegetation degradation [6,7] have become increasingly frequent, severely threatening the stability and functionality of ecosystems and posing substantial challenges to the sustainable development of human society. The Qinghai–Tibet Plateau, known as the "Roof of the World" and the "Third Pole of the Earth", is profoundly affected by global changes due to its unique geographical location and the complexity of its ecosystems [8–11]. The Diqing Tibetan Autonomous Prefecture, which is situated in the transitional zone between the Qinghai–Tibet Plateau and the Yunnan–Guizhou Plateau and lies within the ecological barrier zone of the upper reaches of the Jinsha and Lancang Rivers and characterized by "Three Parallel Rivers" and the confluence of the two major rivers, exhibits highly diverse and complex topographical and climatic conditions, with the quality of the ecological

and environment playing a crucial role in maintaining the regional ecological balance. Systematic research on the spatiotemporal dynamics and driving forces of the ecological environmental quality in the Diqing Prefecture can not only reveal the patterns of ecological change in the region and provide scientific evidence for local ecological protection and resource management, but also serve as a reference for studies in other plateau regions.

The recent advances in environmental monitoring technologies have led to remote sensing techniques gaining widespread application for the monitoring and assessment of ecological and environmental changes due to their efficiency and accuracy [12–15]. Remote-sensing methods capture the dynamic changes in ecosystems on large scales and over long periods, providing robust support for scientific research and environmental management. The remote sensing ecological index (RSEI), a comprehensive evaluation tool, integrates key ecological indicators such as greenness, humidity, heat, and dryness into a unified index through principal component analysis (PCA) [16]. Due to its ability to effectively consolidate various ecological indicators for comprehensive assessment of the ecological environment, RSEI has been successfully applied to ecological environment assessments across different regions and scales, providing scientific evidence for the quantitative analysis of environmental conditions [17–19]. This tool not only aids researchers in gaining a more accurate understanding of the current state and trends of ecological environments, but also offers valuable insights for policymakers in environmental management and decision-making.

Machine learning (ML) has also become a crucial tool in ecological research [20–22]. The ability of ML to capture complex nonlinear relationships unveils hidden patterns and connections that traditional methods often fail to detect, offering unparalleled advantages for explaining the drivers of ecosystem dynamics [19,23–26]. However, despite the strong performance, ML models are often viewed as "black-box" because their decision-making processes are difficult to explain [27]. This issue is particularly challenging in ecological and environmental research, where it is essential to develop the specific roles of driving factors so that effective management strategies are understood. The Shapley additive explanations (SHAP) method offers distinct advantages in this regard [28]. SHAP, which is based on game theory, provides both global and local interpretations of ML models, revealing the internal decision-making logic, highlighting the interactions between complex ecological drivers, and elucidating the predictions made by complex models in understanding how the different variables contribute to these interactions [29–31]. Unlike traditional "black-box" models, SHAP offers a transparent framework that renders decisions more interpretable and reliable, which is particularly important for unraveling the driving forces behind the RSEI.

This study not only evaluates the changes in ecological quality in the Diqing Tibetan Autonomous Prefecture by analyzing long-term trends in the RSEI but also explores the dynamic evolution of the ecological environment of the region in greater detail. ML techniques were combined with SHAP to interpret the key driving factors that bring about these changes, revealing the ecological change patterns in the Diqing Prefecture and providing scientific support for regional ecological conservation and resource management.

2. Materials and Methods

2.1. The Study Area

The Diqing Tibetan Autonomous Prefecture (Figure 1) is located at the heart of the Hengduan Mountains, where the provinces of Yunnan, Sichuan, and Xizang Autonomous Region, and is known for the Three Parallel Rivers, which are considered a natural wonder [32]. The terrain in Diqing resembles a butterfly with its complex geological structure comprising higher elevation in the north and lower elevation in the south. The landscape is predominantly mountainous and features ancient plateau surfaces and ridge peaks, with the Meili Snow Mountain, Yunling Snow Mountain Range, and Shangri-La Snow Mountain Range and the Lancang and Jinsha Rivers flowing between them, forming the well-known "Three Mountains Flanking Two Rivers" geography. The area is home to several national nature reserves, providing crucial ecological services, such as biodiversity conservation

and water resource protection, that serve as a valuable ecological buffer for both local and downstream regions.

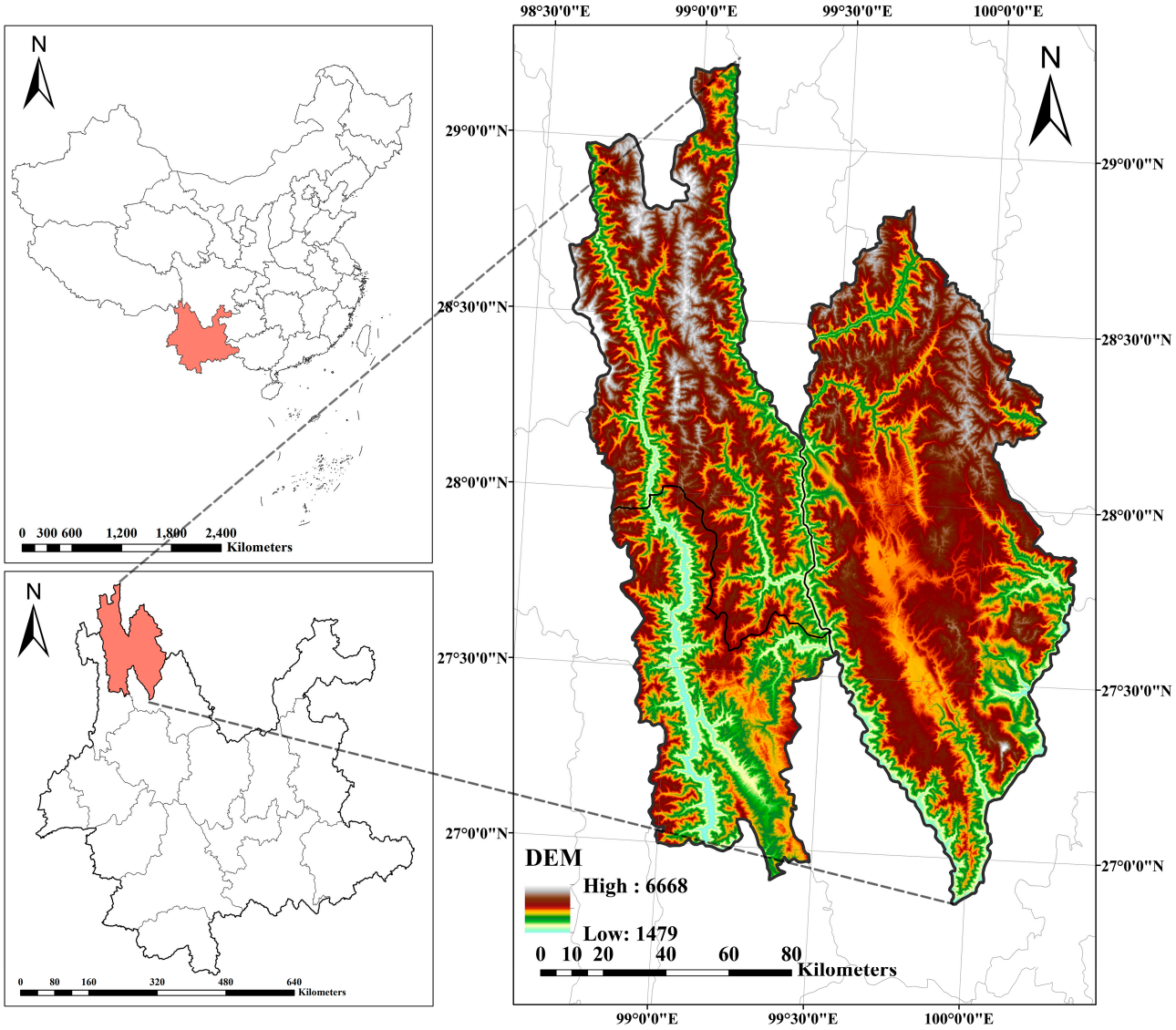


Figure 1. Location of Diqing Prefecture (map source: National Geomatics Center of China; review drawing number: GS (2024) 0650).

The Diqing Prefecture has experienced rapid economic growth in recent years. The burgeoning population and accelerated urbanization have led to an increasing impact on the natural ecosystems in the region, and while rapid development has brought economic prosperity, it also poses significant challenges to the environment. Achieving this balance will not only help safeguard the ecological security and biodiversity of the region but will also promote sustainable economic growth and social stability [33]. These characteristics render the Diqing Prefecture a typical case for the study of ecological protection and economic development in the rapidly urbanizing mountainous regions of southwestern China.

2.2. RSEI Calculation for the Study Area

Moderate-resolution imaging spectroradiometer (MODIS) images have been widely used to monitor ecological conditions on large regional scales. According to the RSEI framework proposed by Xu [16], the four ecological components—greenness, humidity, dryness, and heat—can be described via the normalized difference vegetation index (NDVI), wetness index (WET), normalized difference build-up and soil index (NDBSI), and land

surface temperature (LST), respectively. Three types of MODIS version 6 (V6) datasets were used to obtain the four indicators: the terra vegetation indices product (MOD13A1) for NDVI (500 m spatial resolution and 16-day temporal resolution), the terra surface reflectance product (MOD09A1) (500 m spatial resolution and 8-day temporal resolution) for WET and NDBSI, and the terra land surface temperature and emissivity product (MOD11A2) for LST (1000 m spatial resolution and 8-day temporal resolution). To minimize the uncertainties caused by seasonal variation, MODIS images from the long season (May to September) during the period 2001 to 2021 were selected. The maximum value composite method was used to merge the MOD13A1 NDVI dataset, while for the MOD09A1 dataset, the cloud cover was removed using the quality layer to synthesize high-quality images for the calculation of WET and NDBSI. The LST was derived from the MOD11A2 time series, a product that has undergone various corrections and processing and thus ensures high accuracy and broad coverage while eliminating the effects of cloud and rain conditions. To avoid interference, water bodies were removed from the principal component loadings using the modified normalized difference water index (MNDWI). All preprocessing of the MODIS images and calculations of the four indices were conducted on the Google Earth Engine (GEE) platform (https://earthengine.google.org, which was accessed on 30 July 2024). The calculation methods for each index are listed in Table 1.

Table 1. Calculation methods used for each index.

Index	Calculation Methods
NDVI	$NDVI = 0.0001 \times \rho_{NDVI}$
LST	$LST = 0.02 \times \rho_{LST_Day_1km} - 273.15$
WET	$W_{\mathrm{ET}} = 0.0001 \times (0.1147\rho_1 + 0.2489\rho_2 + 0.2408\rho_3 + 0.3132\rho_4 - 0.3122\rho_5 - 0.6416\rho_6 - 0.5087\rho_7)$
NDBSI	$BI = \frac{[(\rho_6+\rho_1)-(\rho_2+\rho_3)]}{[(\rho_6+\rho_1)+(\rho_2+\rho_3)]}$ $IBI = \frac{\left[\frac{2\rho_6}{\rho_6+\rho_2} - \left(\frac{\rho_2}{\rho_2+\rho_1} + \frac{\rho_4}{\rho_4+\rho_6}\right)\right]}{\left[\frac{2\rho_6}{\rho_6+\rho_2} + \left(\frac{\rho_2}{\rho_2+\rho_1} + \frac{\rho_4}{\rho_4+\rho_6}\right)\right]}$ $NDBSI = \frac{BI+IBI}{2}$

where ρ_{NDVI} represents the NDVI band from the MOD13A1 dataset; $\rho_{LST_Day_1km}$ represents the LST_Day_1km band from the MOD11A2 dataset; and $\rho_{1\sim7}$ represents the 1~7 bands of the MOD09A1 dataset. The LST dataset has a resolution resampled from 1000 m to 500 m.

2.3. Time Trend Test Method

Sen's slope estimator is a robust nonparametric statistical technique that is commonly used for trend calculations [34] and offers several advantages for the analysis of ecological quality changes, including its nonparametric nature, robustness, flexibility, and intuitiveness. The formula is as follows:

$$\beta_{RSEI} = \mathrm{median}\left(\frac{RSEI_{\mathrm{j}} - RSEI_{\mathrm{i}}}{\mathrm{j} - \mathrm{i}}\right) \quad (1)$$

where β_{RSEI} represents the trend change of the time series, and $RSEI_{\mathrm{j}}$ and $RSEI_{\mathrm{i}}$ represent the mean value of RSEI in time periods i and j ($\forall \mathrm{j} > \mathrm{i}$), respectively.

Sen's slope estimator does not autonomously determine the significance of temporal trends. As a result, the Mann-Kendall test was used to assess the statistical significance of the change trend. This test has been used to identify noteworthy trends in long-term shifts of ecological quality in many studies. Referring to the existing studies [35–37], classification is based on the median slope β and the value of the statistic $|Z|$ at the specified 0.1, 0.05, and 0.001 confidence levels α, as reported in Table 2.

Table 2. Classification of ecological quality trends based on β-value and statistic Z.

β	Z	Trend Characteristics	Instructions
$\beta > 0.0005$	$2.58 < \lvert Z \rvert$	Extremely significantly improved	Passes 99% significance test
	$1.96 < \lvert Z \rvert \leq 2.58$	Significantly improved	Passes 95% significance test
	$1.65 < \lvert Z \rvert \leq 1.96$	Mildly improved	Passes 90% significance test
	$\lvert Z \rvert \leq 1.65$	Not significantly improved	Failed the test of significance
$\lvert \beta \rvert \leq 0.0005$	$\lvert Z \rvert$	Unchanged	No significant change
$\beta < -0.0005$	$\lvert Z \rvert \leq 1.65$	Not significantly degraded	Failed the test of significance
	$1.65 < \lvert Z \rvert \leq 1.96$	Mildly degraded	Passes 90% significance test
	$1.96 < \lvert Z \rvert \leq 2.58$	Significantly degraded	Passes 95% significance test
	$2.58 < \lvert Z \rvert$	Extremely significantly degraded	Passes 99% significance test

2.4. Driver Analysis

2.4.1. Driver Selection

To explore the driving forces behind the changes in RSEI, a range of factors encompassing both the natural environmental and the socioeconomic influences were selected as indices, as seen in Table 3. To reduce the informational redundancy among the variables and identify the most critical factors, multicollinearity diagnosis was first conducted by eliminating variables with a variance inflation factor (VIF) > 10. Based on the results of the correlation analysis, only variables with a correlation coefficient $\lvert R \rvert < 0.8$ were retained. The final selected feature variables are listed in Table 3. A 3 km^2 hexagonal grid was used to extract the average values for all feature variables, and the RSEI was used to study changes in the forces driving any changes.

Table 3. Natural environmental and socio-economic factors.

Indicators	Data Sources
Precipitation (PRE)	1-km monthly precipitation dataset for China (1901–2023). National Tibetan Plateau/Third Pole Environment Data Center [38]. https://doi.org/10.5281/zenodo.3114194.
Total evapotranspiration (ET)	MODIS/Terra Net Evapotranspiration Gap-Filled 8-Day L4 Global 500 m SIN Grid V061 [dataset]. NASA EOSDIS Land Processes Distributed Active Archive Center [39]. Accessed on 5 August 2024 from https://doi.org/10.5067/MODIS/MOD16A2GF.061
Soil moisture (SM)	A 1 km daily soil moisture dataset over China based on in-situ measurement (2000–2022). National Tibetan Plateau/Third Pole Environment Data Center [40]. https://doi.org/10.11888/Terre.tpdc.272415. https://cstr.cn/18406.11.Terre.tpdc.272415 (accessed on 5 August 2024).
Fraction of absorbed Photosynthetically active radiation (FPAR)	A high-quality reprocessed MODIS fraction of absorbed photosynthetically active radiation dataset (HiQ-FPAR) (Version 1) [dataset] [41]. Zenodo. https://doi.org/10.5281/zenodo.10683549.
Relative humidity (RH)	A first 1 km high-resolution atmospheric moisture index collection over China, 2003–2020 [42]. National Tibetan Plateau/Third Pole Environment Data Center. https://doi.org/10.5281/zenodo.8070140.
Digital elevation model (DEM)	NASADEM Merged DEM Global 1 arc second V001 [dataset]. NASA EOSDIS Land Processes DAAC [43]. https://doi.org/10.5067/MEaSUREs/NASADEM/NASADEM_HGT.001
Gross domestic product (GDP)	The Spatial Distribution of China's GDP: Kilometer-Grid Dataset [44] (http://www.resdc.cn/DOI, accessed on 5 August 2024), 2017. https://doi.org/10.12078/2017121102.
Human footprint (HF)	An annual global terrestrial human footprint dataset from 2000 to 2018 [45] (https://doi.org/10.6084/m9.figshare.16571064).

2.4.2. Machine Learning Algorithm

CatBoost [46], which was recently developed by Yandex, is a highly efficient algorithm that is based on Gradient Boosting Decision Tree (GBDT). CatBoost utilizes a symmetric tree structure and enhances the efficiency of both model training and prediction while simultaneously reducing the memory consumption. CatBoost has a variety of hyperparameters that pose a non-negligible effect on model performance.

The numerous hyperparameters in CatBoost mean that optimizing the parameters of the model through the grid search method is difficult and costly in terms of computational power. Consequently, a CatBoost hyperparameter tuning approach that integrates Bayesian optimization with 5-fold cross-validation was employed. This method facilitates the rapid identification of globally optimal model configurations within the parameter space, ensuring model generalization while mitigating the risk of overfitting. All parameter optimizations were performed with the 2020 dataset, using the following optimization parameters: 'iterations'—1291, 'depth'—9, 'learning_rate'—0.04, and 'l2_leaf_reg'—0.004. The rest of the hyperparameters were left as default.

The final modeling process involved dividing the data into 80% for the training set and 20% for the validation set. The CatBoost regression method, implemented in version 1.2.5 of the CatBoost library in Python version 3.8 [47], was utilized with three metrics: R^2, mean absolute error (MAE), and root mean square error (RMSE) employed to evaluate the performance of the CatBoost models and ensure the reliability of the analysis.

2.5. Interpretation of Drivers Using SHAP Analysis

Advanced machine learning models often outperform the traditional linear statistical models in terms of accuracy and generalization. However, one key drawback is that these algorithms often produce predictions that are difficult to interpret; this is known as the "black-box problem" in machine learning [27]. To address this issue, the SHAP algorithm was used to identify the nonlinear effects of the socio-ecological drivers on the RSEI [28]. Based on game theory, SHAP assigns an interpretability score to each feature by calculating its contribution to the predictions made by a model. The calculation of a SHAP value relies on the concept of Shapley values, which assess the impact of each feature by considering all possible feature value combinations. SHAP analysis helps rationalize model predictions and contextualize explanations for the outcomes of a model.

The formula for the SHAP value of feature i is as follows:

$$\phi_i = \sum_{S \subseteq F \setminus \{i\}} \frac{|S|!(|F|-|S|-1)!}{|F|!} [f(S \cup \{i\}) - f(S)] \quad (2)$$

where ϕ_i represents the SHAP value for feature i, indicating the importance of feature i for the prediction of the model; and S is a subset of features that are selected from the entire set F, where F is the set of all features. The function $f(S \cup \{i\})$ is the model trained on the feature subset $S \cup \{i\}$, which includes feature i; $f(S)$ is the model trained on the feature subset S excluding feature i; $|S|$ denotes the number of features in subset S; and $|F|$ is the total number of features in set F.

SHAP measures the pairwise interaction effect of feature i and j is given by the following:

$$\phi_{i,j} = \frac{1}{2} \sum_{S \subseteq F \setminus \{i,j\}} \frac{|S|!(|F|-|S|-2)!}{|F|!} [f(S \cup \{i,j\}) - f(S \cup \{i\}) - f(S \cup \{j\}) + f(S)] \quad (3)$$

where $\phi_{i,j}$ represents the SHAP interaction value between features i and j.

For a given input sample z with M explanatory variables, an explanation model g is expressed as a linear function of feature contributions as follows:

$$g(z') = \phi_0 + \sum_{i=1}^{M} \phi_i z_i' \quad (4)$$

where $g(z')$ represents the output of the additive explanation model; ϕ_0 denotes the base value; ϕ_i is the SHAP value of the feature i; z_i' is a binary indicator variable for feature i, if $z_i' = 1$, it means that feature i is included in the model, if $z_i' = 0$, the feature is excluded; and M denotes the total number of features in the model. The SHAP approach used in this study was implemented using version 0.44.1 of the Python SHAP library [28], along with Python version 3.8.

3. Results

3.1. RSEI Calculation Results

The results of the principal component analysis (Figure 2) indicated that the combined contribution of the first and second principal components in each year exceeded 80%. Band math was used to weight and average out the two principal components, and the results were used to ascertain the RSEI values for the Diqing Prefecture.

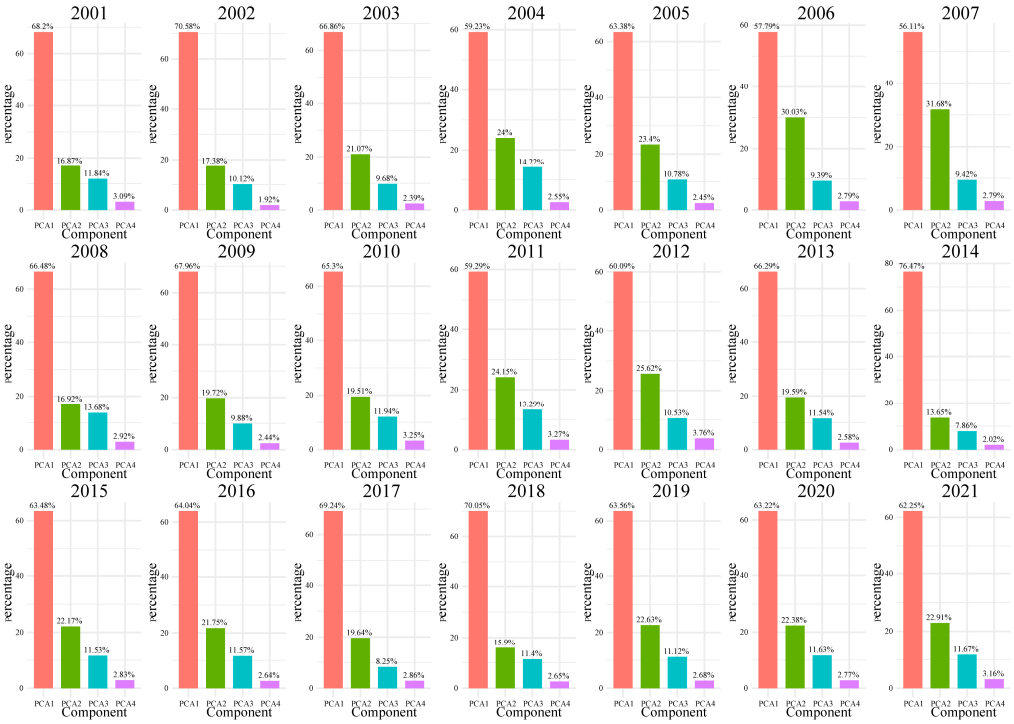


Figure 2. Principal component contributions from 2001 to 2021.

Our results show that the mean values of the validation metrics for the CatBoost model, averaged over four years, gradually improved after the optimization (Table 4). The modeling results that were based on the CatBoost model demonstrated exceptional predictive performance, with the R^2 values for the training dataset remaining consistently high in all years, particularly 2005, when the model achieved an R^2 of 0.9138. The obtained results indicate the excellent capability of the model to capture the complexity of ecological index changes. The R^2 values for all test sets were greater than 0.7, indicating the overall good performance of the model. Moreover, the low RMSE and MAE values in the testing set confirmed the predictive accuracy and applicability of the model. These results indicate that the constructed CatBoost model can effectively adapt to and predict spatiotemporal

changes in the ecological index, thereby providing a solid foundation for ecological analysis with high reliability and precision.

Table 4. Comparison of statistics for model evaluation.

		Before Optimization			After Optimization		
		R^2	MAE	RMSE	R^2	MAE	RMSE
2005	Training dataset	0.9046	0.0340	0.0447	0.9138	0.0317	0.0425
	Testing dataset	0.8281	0.0456	0.0608	0.8270	0.0459	0.0610
2010	Training dataset	0.8529	0.0479	0.0642	0.8787	0.0420	0.0583
	Testing dataset	0.7496	0.0617	0.0839	0.7454	0.0620	0.0846
2015	Training dataset	0.8242	0.0479	0.0629	0.8424	0.0442	0.0595
	Testing dataset	0.7040	0.0611	0.0799	0.7035	0.0607	0.0800
2020	Training dataset	0.8226	0.0483	0.0635	0.8364	0.0452	0.0610
	Testing dataset	0.7295	0.0587	0.0778	0.7330	0.0583	0.0773
	Mean value	0.8019	0.0507	0.0672	0.8100	0.0488	0.0655

3.2. Ecological Quality Changes in the Diqing Prefecture

The temporal variations in the average RSEI values within the study area can be seen in Figure 3. The trend observed in the mean RSEI curve indicates a general upward fluctuation in the RSEI of the Diqing Prefecture from 2001 to 2021, with the increase in the mean value from 0.44 in 2001 to 0.71 in 2021 suggesting an overall improvement in the ecological quality. Significant fluctuations were observed in the mean RSEI throughout the period, with the maximum of 0.71 in 2006 followed by a decline to 0.59 and 0.57 in 2009 and 2010, respectively. The lowest point of 0.51 in 2017 was followed by a gradual recovery, with a mean RSEI of 0.71 observed in 2021. The trend analysis assessed the overall variation in the time series of the mean RSEI values, indicating an upward trend in the RSEI. The orange curve, smoothed using the Savitzky–Golay filter, mitigates these short-term fluctuations and reveals an upward long-term trend for the RSEI in the study area over the observation period [19].

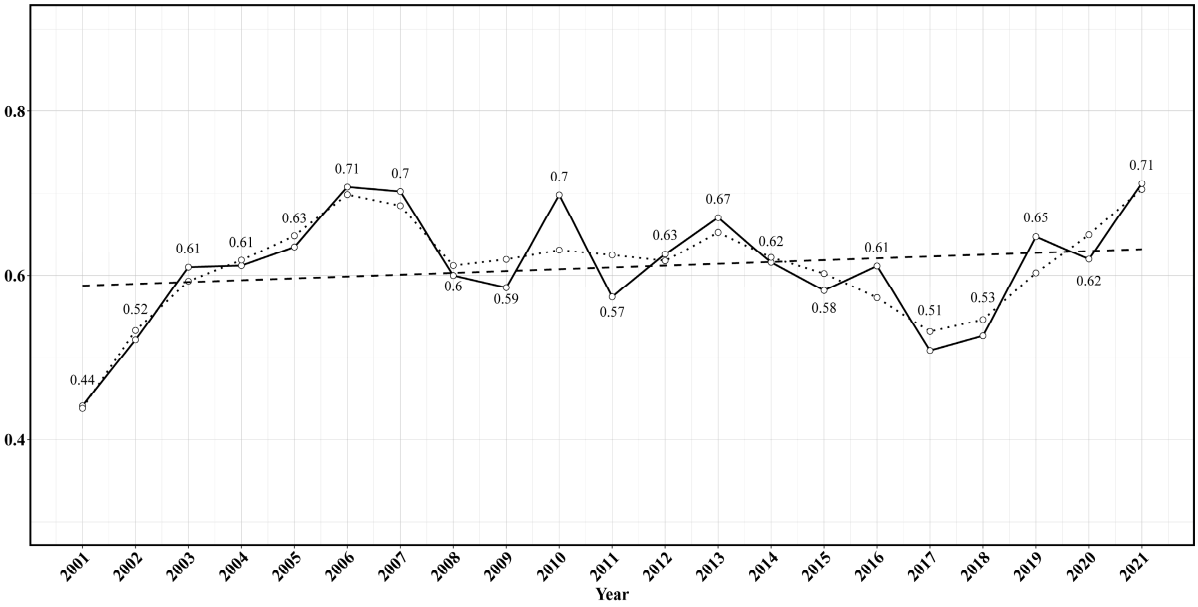


Figure 3. Time series change in the average RSEI in the study area from 2001 to 2021. The solid line represents the mean change in RSEI, the dotted line depicts the changes following SG filter smoothing, and the dashed line illustrates the trend in RSEI changes.

As seen in Figure 4, the ecological quality in the Diqing Prefecture from 2001 to 2021 was predominantly "good", accounting for 42.77 ± 2.72%, followed by "moder-

ate" at 21.93 ± 1.23% and "excellent" at 16.62 ± 2.40%. The "fair" level accounted for 16.11 ± 2.15% and the "poor" level for only 2.57 ± 0.51% of the total, indicating an overall improvement in the ecological quality of the region. The spatial distribution of the RSEI in 2001 showed that areas with poorer ecological quality were mainly located in mid-to-high-altitude mountainous regions and along riverbanks. However, the RSEI values in these areas exhibited a fluctuating upward trend over time, particularly in 2010 and 2021, when large areas in the southwestern and eastern regions were classified as "excellent", and only localized high-altitude areas showed lower ecological quality. This indicates a significant improvement in the ecological quality of the Diqing Prefecture during the study period.

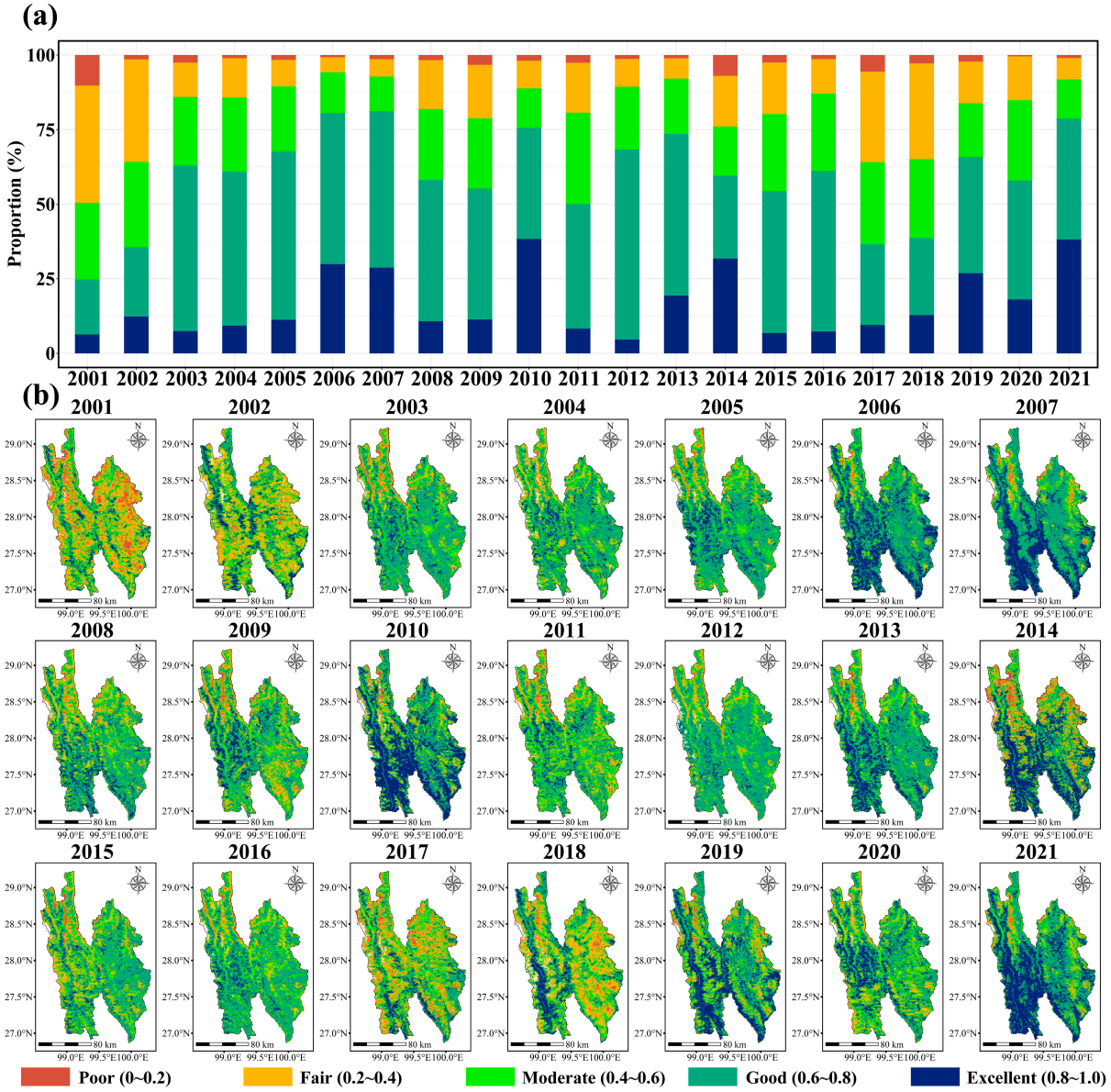


Figure 4. Annual ecological quality in the study area from 2001 to 2021; (**a**) inter-annual changes in the mean RSEI and the proportion of RSEI in each level; (**b**) spatial distribution of the RSEI level.

3.3. Spatial and Temporal Trends in Ecological Quality

Both Sen's slope and the Mann–Kendall test were used to analyze the spatial trends in the RSEI. The results were divided into nine categories: extremely significant improvement, significant improvement, mild improvement, non-significant improvement, unchanged, extremely significant degradation, significant degradation, mild degradation, and non-significant degradation. The results showed that the RSEI in the study area primarily

exhibited a non-significant improvement trend (58.66%) across most of the Diqing Prefecture from 2001 to 2011, followed by a non-significant degradation trend (21.78%) and a mild increasing trend (7.65%), as seen in Figure 5. The areas with mild and above improvement trends were distributed sporadically across most of Diqing, whereas the non-significant degradation trends were mainly concentrated in the northwest, central low-altitude valleys, and along the riverbanks. The RSEI continued to show a non-significant improvement trend (53.64%) from 2011 to 2021, predominantly in the mid-to-low-altitude areas of Diqing, followed by a non-significant degradation trend (29.14%), which occurred primarily in the high-altitude mountainous regions. Significant degradation trends (0.7%) were also observed in high-altitude areas. Mild and high improvement trends were mainly concentrated in the low-altitude valleys and along riverbanks in the western and northeastern parts of the region. Considering the long-term trend, the RSEI showed a non-significant improvement trend (55.17%) across most of the Diqing Prefecture from 2001 to 2021, with areas demonstrating declining ecological quality concentrated in the high-altitude mountainous regions and the improvement trends along the Lancang River in the southwest. Overall, these results indicate an upward trend in the ecological quality across the Diqing Prefecture during the study period.

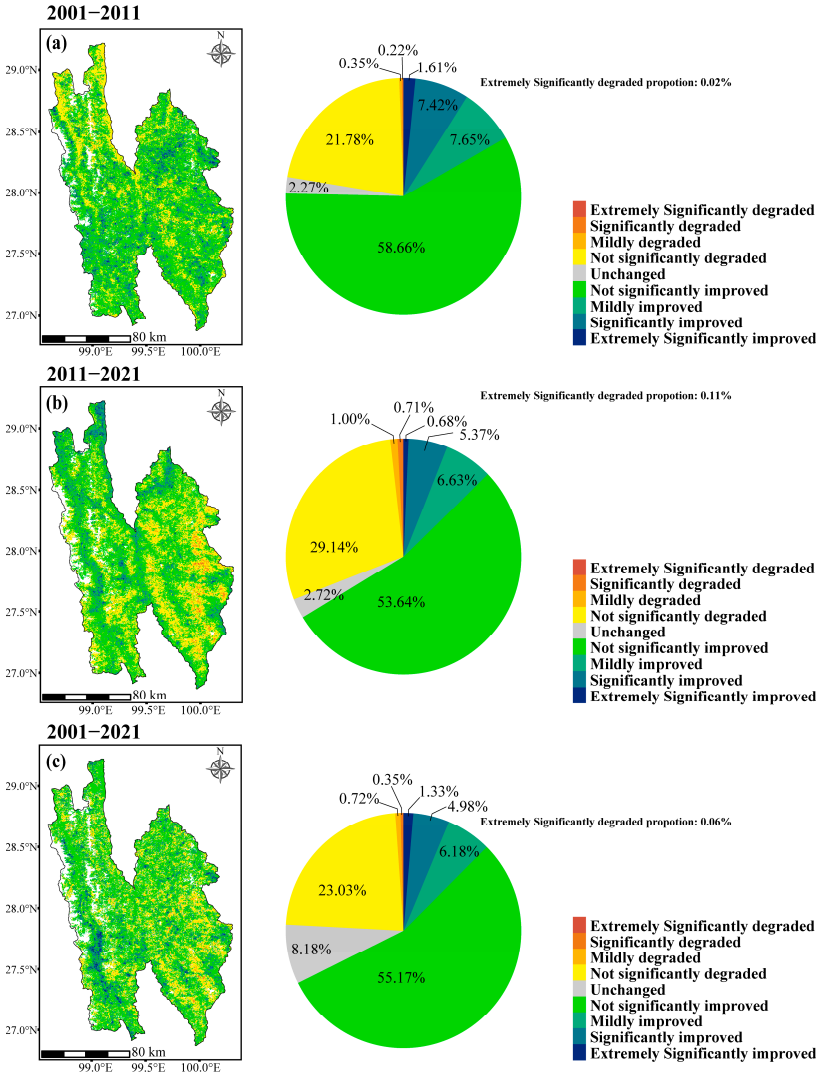


Figure 5. Distribution of different spatial trends in the RSEI and the proportion of area occupied by each. (**a**) Spatial trends of the RSEI and the proportion of area from 2001 to 2011; (**b**) Spatial trends of the RSEI and the proportion of area from 2011 to 2021; (**c**) Spatial trends of the RSEI and the proportion of area from 2001 to 2021.

3.4. Changes in the Drivers of the ERSI in Diqing

The changing trends in the RSEI drivers across the different years can be seen in Figure 6. FPAR was the most significant driver in 2005, 2015, and 2020, whereas the DEM dominated in 2010, with lower contributions in other years. FPAR exhibited the most significant positive impact on SHAP values, with higher feature values (deeper red) corresponding to higher positive SHAP values, indicating a positive feedback loop between RSEI and FPAR. FPAR had a strong marginal positive influence on the probability of RSEI prediction, with ET, RH, and ASPECT showing similar trends across the 4 years. The distribution of all other driver factors, represented by the blue and red points, lacked a consistent pattern, suggesting that the correlation between these drivers and RSEI is not as simple as a positive/negative trend.

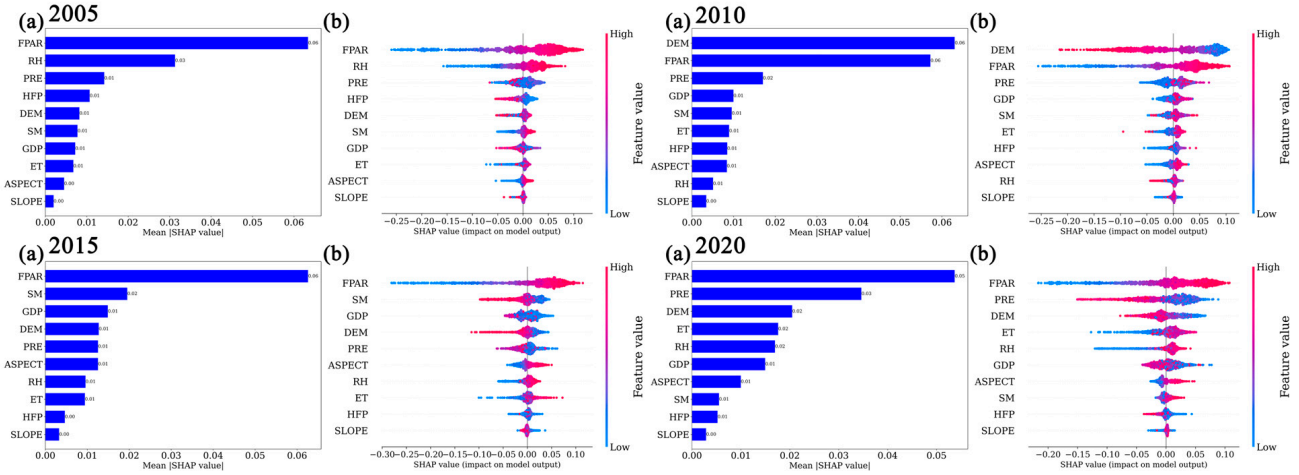


Figure 6. SHAP value obtained using the Catboost regression model for RSEI and ten natural anthropogenic drivers. (**a**) Average of absolute SHAP values; (**b**) SHAP values obtained for each driver. PRE = precipitation; ET = total evapotranspiration; SM = soil moisture; FPAR = fraction of absorbed photosynthetically active radiation; RH = relative humidity; DEM = digital elevation model; GDP = gross domestic product; and HF = human footprint.

The SHAP dependency plots for all socio-ecological factors can be seen in Figure 7, while the interaction effects between the top five variables and the DEM are given in Figures 8 and 9. FPAR exhibited a consistent linear increase in SHAP values across the different years, with a more pronounced effect on the RSEI in mid-to-high-altitude regions.

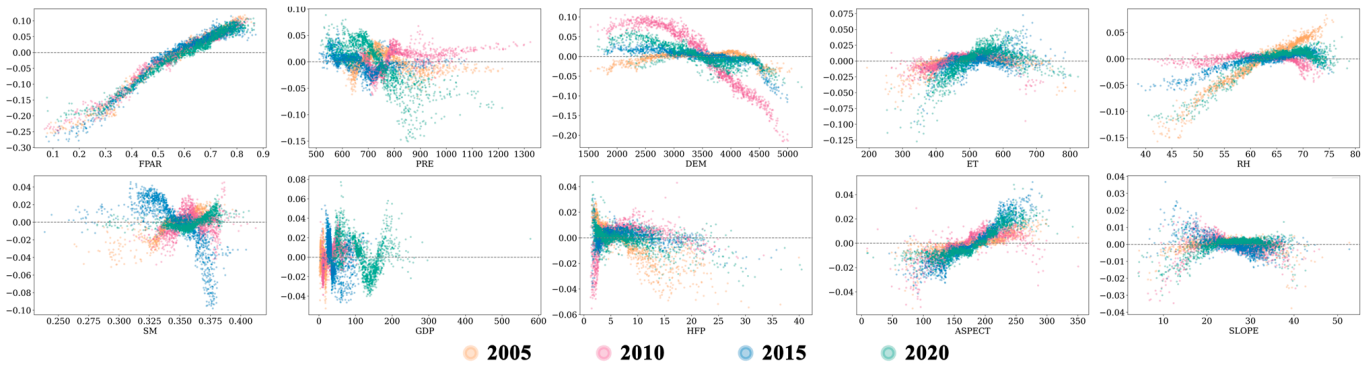


Figure 7. SHAP values showing the effects of ten natural anthropogenic environment variables on the RSEI.

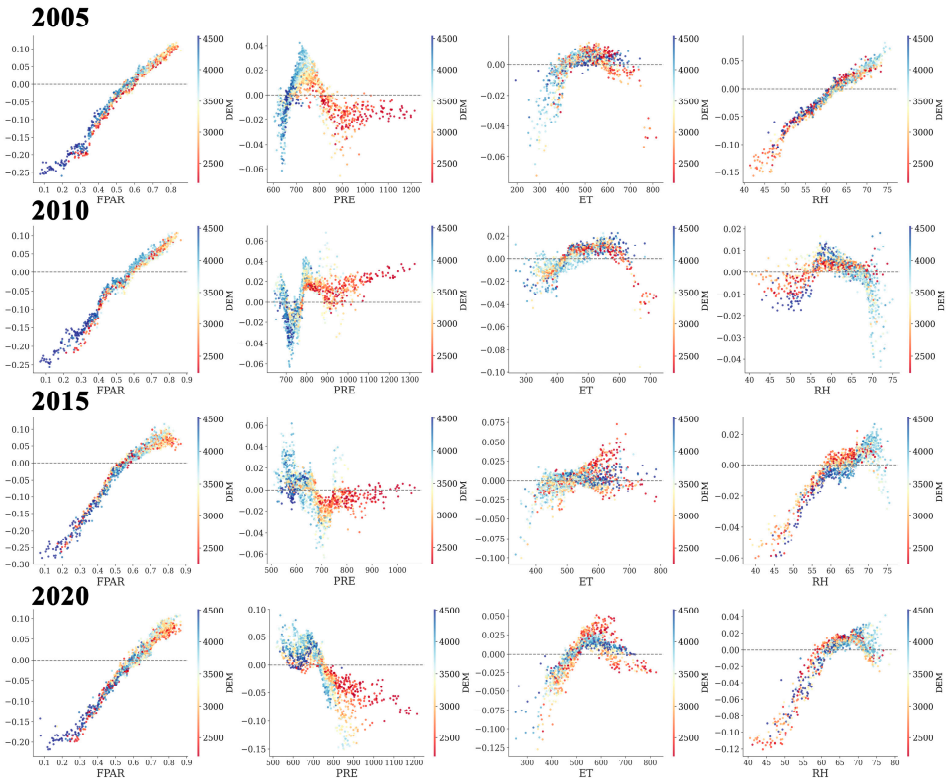


Figure 8. SHAP dependency graph showing the interaction effects between environment variables (FPAR, PRE, ET, and RH) and the DEM.

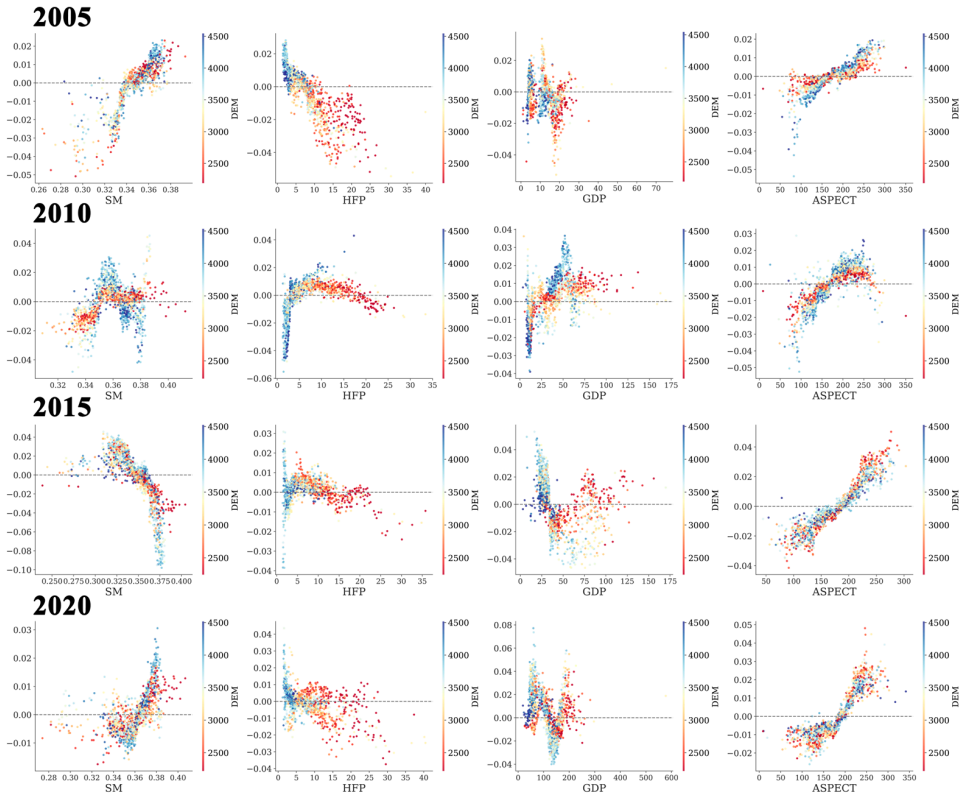


Figure 9. SHAP dependency graph of the interaction effects between environment variables (SM, GDP, HFP, and ASPECT) and the DEM.

The increased precipitation (PRE) in 2015 and 2020 led to a change in the SHAP values from positive to negative, indicating that precipitation positively impacts the RSEI under lower precipitation conditions (500–700 mm) and negatively affects the RSEI when precipitation exceeds 700 mm. The low precipitation in 2005 negatively impacted the RSEI, disappearing when precipitation reached 800 mm. However, the low precipitation in 2015 (<700 mm) led to a positive effect, followed by a decrease in the effect, and then a fluctuating upward trend. Precipitation in low-altitude areas is generally higher than in high-altitude regions.

The SHAP values for ET exhibited a hump-shaped trend. In the lower range (200–400 kg/m^2), ET had a negative impact on the RSEI. However, its impact gradually became more positive as the ET exceeded 400 kg/m^2, with further increases resulting in negative effects. The SHAP values showed significant differences across the years, with moderate ET generally having a positive impact on the model. The greatest variability was observed in 2020, whereas the influence of ET on RSEI in 2015 was more dispersed. The threshold for the positive impact of evapotranspiration on the RSEI was higher in 2015 and 2020 (approximately >500 kg/m^2). The impact of evapotranspiration on RSEI was generally more significant in low-altitude areas.

RH had a significant positive effect on the RSEI in 2005, 2015, and 2020, when it exceeded 60%, mainly at altitudes below 4500 m. However, the higher RH (>70%) in 2010, 2015, and 2020 negatively impacted the RSEI.

High SM levels in 2005 (>0.34 m^3/m^3) and 2020 (>0.36 m^3/m^3) resulted in a positive impact on the RSEI, while higher moisture levels had a significant negative effect in 2015 (>0.35 m^3/m^3), with more pronounced effects observed in mid-to-high-altitude areas. The impact of soil moisture on the RSEI exhibited a fluctuating trend in 2010, with low soil moisture in low-altitude areas and high soil moisture in high-altitude areas negatively affecting the RSEI. Moderate moisture levels had a positive impact on the RSEI, with mid-to-high-altitude areas showing more significant positive effects under these conditions.

Low HFP values were mainly observed in mid-to-high-altitude areas, and the impact of HFP on the RSEI varied across the years, with HFP impacting the RSEI positively in 2005 and 2020 and negatively in 2010. Both positive and negative effects were observed in 2015. Moderate HFP levels had a positive effect on RSEI in mid-to-low-altitude areas and a significant negative impact in mid-to-low-altitude regions, with the negative impact in low-altitude areas becoming more pronounced as the HFP increases.

The impact of GDP on the RSEI exhibited fluctuating trends across different years, with higher impacts observed in high-altitude areas than in low-altitude areas with the same GDP levels. The SHAP values for ASPECT generally showed an upward trend, with a higher slope being more favorable for the RSEI. The impact of ASPECT on RSEI varied across years, with more dispersed effects observed in 2005 and 2010, including negative impacts in some regions. However, the impact of ASPECT became more consistent in 2015 and 2020, when it showed a more significant positive trend.

The DEM had a notable negative impact on the RSEI in 2010, 2015, and 2020. Increasing elevation led to a decrease in the RSEI, with DEM having a positive effect below approximately 3500 m and a negative impact above 3500 m. The differences in the impact that the DEM had on the RSEI across the 3 years were mainly due to the magnitude of the changes. In 2005, the DEM showed an inverted U-shape trend, with elevations below approximately 2500 m and above 4500 m showing negative effects on the RSEI and other areas showing positive effects.

SLOPE showed a relatively small impact on the RSEI, with most SHAP values concentrated near zero, indicating limited contribution of the slope to the ecological quality. A divergent trend was observed across all years in the lower slope range (0–20°), the SHAP values tended to be less than zero across all years in the higher slope range (30–50°).

4. Discussion

4.1. Trends in the RSEI Changes in the Diqing Prefecture

Analysis of the RSEI trends in the Diqing Prefecture from 2001 to 2021 revealed a dynamic evolution of the ecological quality in the region. Overall, the RSEI values in the Diqing Prefecture exhibited a fluctuating upward trend over the last two decades, indicating significant improvement in the ecological quality, albeit under the influence of various complex factors. The marked fluctuations in the RSEI values during certain years reflect the profound impact of climate change on the ecosystem. For instance, in 2006, the RSEI peaked at 0.71 and then declined to 0.59 in 2009 and 0.57 in 2011, with the fluctuations likely related to severe droughts in 2009 and 2011. Research has shown that these drought events significantly reduce the net primary productivity (NPP) in the southwestern region [48], severely inhibiting the growth of vegetation and substantially decreasing carbon sequestration. Droughts also negatively affect the soil moisture [49–51], further impairing vegetation recovery capacity and reducing the overall ecological quality. Despite these challenges, the RSEI began to recover gradually in 2018, attaining a height of 0.71 in 2021 that indicated a certain level of resilience in the regional ecosystem.

Human activities are also significant drivers of changes in RSEI. Studies have shown that grazing practices in the Qinghai–Tibet Plateau region can have substantial impacts on alpine grasslands [8,52]. The implementation of ecological engineering projects has played a crucial role in improving ecological quality in the Diqing Prefecture [53,54] China implemented the Natural Forest Protection Project on 1 September 1998, and since then the Diqing Prefecture has adopted a development strategy centered on "ecological governance", rendering ecological environment protection and construction the impetus of forestry in the region. The Grain for Green Project was launched in the Diqing Prefecture in 2002, with the first phase covering more than 300,000 mu, while the "Diqing Tibetan Autonomous Prefecture Ecological Prefecture Construction Plan" was implemented at the beginning of 2013, marking a new chapter in eco-environmental conservation. During the 13th Five-Year Plan period (2016–2020), the forest coverage rate in the Diqing Prefecture has increased from 75.03% to 76.58% and the forest stock volume from 257 to 268 million m^3. The comprehensive implementation of the Natural Forest Protection Project effectively protected 1.9093 million ha of natural forest across the prefecture. Additionally, 5500 ha of afforestation in rocky desertification areas, 41,500 ha of forest enclosures, 20,000 ha of low-efficiency forest renovation (including forest tending projects), and 9500 ha of the new Grain for Green Project have been completed. The region has also planted 13.83 million voluntary trees, with 574,000 seedlings in the reserves. Moreover, the implementation of the Grazing to Grassland Project affected 43,300 ha, and the Grassland Ecological Restoration and Management Project covered 3300 ha, with 1.7671 million ha of public welfare forests protected. Previous research has shown that ecological restoration projects have led to a significant increase in NDVI on the Qinghai–Tibet Plateau (QTP) and that vegetation recovery has contributed to the enhancement of various ecosystem services on the QTP [55]. Our research also suggests that ecological conservation, restoration, and greening projects have improved the ecological quality of the Diqing Prefecture. To achieve environmental protection without sacrificing socio-economic development, the Diqing Prefecture has delineated ecological protection red lines [56]. These red lines are defined as spatial boundaries and management limits that require strict protection in areas crucial for national and regional ecological security, sustainable economic and social development, and public health [57]. The red lines delineate areas that must be protected in terms of natural ecological services, environmental quality safety, and natural resource use. Within these red lines, strict supervision will be enforced, with development and production activities prohibited. Limited human activities that do not damage ecological functions are allowed only in accordance with laws and regulations. Meanwhile, the Chinese government is actively promoting ecological compensation to balance economic development and environmental protection [58]. The ecological compensation mechanism in the Diqing Prefecture has been continuously tested and developed in practice [59].

4.2. Changes in the Drivers of RSEI in the Diqing Prefecture

The CatBoost-SHAP framework was used to explore changes in the ecological and socioeconomic drivers in the Diqing Prefecture across different years. Comparative analysis indicated that the contribution rates of these drivers varied significantly across the study period. Natural climatic factors had a greater influence than socioeconomic factors, and the impact of certain drivers on the RSEI varied significantly in different years. This variation is primarily due to the effects of climate change and environmental fluctuation, as climatic conditions often differ greatly from year to year, directly affecting the state of the ecosystem. Research has shown that the ecological stability of the Qinghai–Tibet Plateau is relatively low [60]. Vegetation in the area is highly sensitive to climate change, with the NDVI of the plateau grasslands showing an overall declining trend from 2000 to 2015, driven by reduced precipitation and rising temperatures [8].

Additionally, dynamic changes within the ecosystem itself can influence the contribution rates and sources of impact from the underlying drivers. Ecosystems often exhibit a resistance–resilience chain response to climate change [61–63], where the impact of certain drivers in specific years may become more pronounced or diminished owing to the self-regulation of an ecosystem. Studies have shown that severe precipitation deficits can suppress vegetation growth and ecosystem productivity on the Qinghai–Tibet Plateau. However, plant growth and productivity have been observed to rapidly recover during subsequent periods of rewetting [64]. Our research indicates that in the Diqing Prefecture, while the region faced the impact of drought in 2009, the higher precipitation in 2010 had a positive effect on the RSEI (Figures 6 and 8), whereas the increased precipitation in other years tended to have a negative impact.

Land use change and the intensity of human activities are the key factors that influence the contribution rates of drivers. Studies have shown that grazing has a significant negative impact on the alpine grasslands of the Qinghai–Tibet Plateau [8,52]; however, various ecological projects on the plateau have already achieved considerable success in restoring vegetation in the area [63], thus offsetting the effect of extensive gazing. Our research also demonstrates that the impact of human footprint (HFP) on the RSEI varies significantly across years, suggesting that the impact of human activities is not uniformly positive or negative: while activities such as grazing and urbanization may lead to ecological degradation at certain times, ecological restoration measures have the potential to gradually enhance ecological quality.

4.3. Interaction Effects of RSEI Drivers in the Diqing Prefecture

By utilizing the CatBoost-SHAP framework to explore the interaction effects between various driving factors and a DEM, we found that the influence of these drivers on the RSEI varied across different altitudes. We hypothesize that this variation is primarily due to the moderating effect of topographical elevation on the ecological and socioeconomic drivers. Research has shown significant topographical effects on the vegetation activity on the Qinghai–Tibet Plateau, with differences in greening isoclines observed at different altitudes [65,66]. In the mountainous canyon regions of southwestern China, elevation was the dominant factor influencing the spatial heterogeneity of NDVI, with the explanatory power reaching 64% [67]. The interaction between dual factors, such as elevation and climate, provided greater explanatory power than single-factor effects. Human activity varies with altitude. Low-altitude areas are typically the focus of human activities such as agricultural development and urbanization, leading to a more pronounced impact from socioeconomic drivers on the RSEI in these areas. In contrast, human activities are relatively sparse in high-altitude areas, and natural factors may play a more significant role in such regions. Studies have shown that in the ecological barrier regions of Sichuan and Yunnan [68], low-altitude areas have been subjected to significant changes in land-use pattern and landscape structure to meet production demands that pose further risks to the ecological environment. In high-altitude regions, where human interference is minimal, the landscape structure remains relatively stable.

4.4. Limitations

Our research still faces numerous issues that require urgent improvement. Firstly, incorporating additional indicators could enhance the calculation of RSEI specific to the Diqing Prefecture, thereby providing a more accurate representation of changes in ecological quality in the region. Secondly, the extent to which the multi-source data used in this study reflects the impact of various driving forces on the RSEI warrants further consideration. For example, the GDP data utilized in this study are derived from a spatial distribution dataset of GDP in China, which is based on county-level GDP statistics. This dataset, which incorporates land use types, nighttime light intensity, and settlement density data, as well as the spatial interaction patterns of GDP, is generated through spatial interpolation to create a 1 km $\times$ 1 km grid. This approach might obscure economic differences within regions; using per capita GDP could potentially offer a more detailed understanding of the relationship between economic development and ecological impact. Moreover, although our study provides a method for exploring the impact of driving forces on RSEI using interpretable machine learning, the significant differences among various machine learning models suggest that comparing a broader range of models and interpretative methods is a crucial step to enhance the scientific rigor of the research. Finally, this study provides only a macro-level understanding of changes in ecological quality and the impact of various driving forces in the Diqing Prefecture, while overlooking more specific issues. For instance, a more nuanced investigation is required to quantify the benefits of ecological protection red lines and ecological compensation mechanisms in terms of their contributions to both ecological preservation and economic development in the Diqing Prefecture.

5. Conclusions

In this study, the spatiotemporal changes in the ecological quality of the Diqing Prefecture from 2001 to 2021 were analyzed using the RSEI, and the CatBoost ML algorithm was combined with the SHAP method to interpret the driving factors and their interactions. The results indicate that the ecological quality in the Diqing Prefecture generally improved over the study period, although this trend was not linear and was influenced by various complex factors. Climate change, particularly extreme weather events such as drought and abnormal precipitation, has had a significant impact on the regional ecological quality, while the implementation of ecological protection projects plays a crucial role in enhancing it.

The analysis of driving factors across different years revealed that natural climatic factors had a greater influence on RSEI than socioeconomic factors, with fluctuations in the climatic conditions causing significant temporal variations in how these drivers impact ecological quality. This result reflects the sensitivity of the Qinghai–Tibet Plateau ecosystem to climate change and the self-regulating capacity of the region. Further analysis of the interactions among the driving factors showed distinct differences in their impact on the ecological quality across different altitudes, with natural drivers being more significant in high-altitude areas and human activities having a greater influence in low-altitude areas.

In summary, this study elucidated the dynamic evolution of the ecological quality in the Diqing Prefecture, emphasizing the combined effects of climate change, human activity, and ecological engineering on the regional ecosystem. Future ecological management should continue advancing and optimizing ecological engineering, particularly in the context of climate change, by strengthening measures such as vegetation restoration, wetland protection, and soil and water conservation. Additionally, high-resolution remote sensing data and advanced ML techniques should be integrated to continuously monitor changes in ecological quality, enabling timely adjustment and improvement to any ecological protection strategies to ensure the sustainable development of the regional ecosystem and the ongoing enhancement of the environmental quality.

Author Contributions: Q.S. and Z.Z. provided funding acquisition, project administration, and resources. C.W. performed the research collection and analyzed and interpreted the data. C.W. wrote

the manuscript with contributions from all co-authors. All authors have read and agreed to the published version of the manuscript.

Funding: This research was funded by the National Natural Science Foundation of China (31770752); the National Natural Science Foundation for Young Scientists of China (32101582); the National Social Science Foundation of China Art Project (22BG110); the Postgraduate Research and Practice Innovation Program of Jiangsu Province (KYCX23_1261); Ministry of Education Humanities and Social Sciences Research "Study on the new mechanism of urban green space ecological benefit Measurement and high-quality collaborative development: A case study of Nanjing Metropolitan Area" (21YJCZH131); Social Science Foundation Project of Jiangsu Province (21GLC002).

Data Availability Statement: All databases (sources and references) are described in Section 2.

Conflicts of Interest: The authors declare no conflicts of interest.

References

1. Bellard, C.; Bertelsmeier, C.; Leadley, P.; Thuiller, W.; Courchamp, F. Impacts of climate change on the future of biodiversity. *Ecol. Lett.* **2012**, *15*, 365–377. [CrossRef] [PubMed]
2. Dawson, T.P.; Jackson, S.T.; House, J.I.; Prentice, I.C.; Mace, G.M. Beyond Predictions: Biodiversity Conservation in a Changing Climate. *Science* **2011**, *332*, 53–58. [CrossRef] [PubMed]
3. Langdon, J.G.R.; Lawler, J.J. Assessing the impacts of projected climate change on biodiversity in the protected areas of western North America. *Ecosphere* **2015**, *6*, art87. [CrossRef]
4. Padrón, R.S.; Gudmundsson, L.; Decharme, B.; Ducharne, A.; Lawrence, D.M.; Mao, J.; Peano, D.; Krinner, G.; Kim, H.; Seneviratne, S.I. Observed changes in dry-season water availability attributed to human-induced climate change. *Nat. Geosci.* **2020**, *13*, 477–481. [CrossRef]
5. Piao, S.; Ciais, P.; Huang, Y.; Shen, Z.; Peng, S.; Li, J.; Zhou, L.; Liu, H.; Ma, Y.; Ding, Y.; et al. The impacts of climate change on water resources and agriculture in China. *Nature* **2010**, *467*, 43–51. [CrossRef] [PubMed]
6. Higgins, S.I.; Conradi, T.; Muhoko, E. Shifts in vegetation activity of terrestrial ecosystems attributable to climate trends. *Nat. Geosci.* **2023**, *16*, 147–153. [CrossRef]
7. Ma, M.; Wang, Q.; Liu, R.; Zhao, Y.; Zhang, D. Effects of climate change and human activities on vegetation coverage change in northern China considering extreme climate and time-lag and -accumulation effects. *Sci. Total Environ.* **2023**, *860*, 160527. [CrossRef]
8. Wang, Y.; Lv, W.; Xue, K.; Wang, S.; Zhang, L.; Hu, R.; Zeng, H.; Xu, X.; Li, Y.; Jiang, L.; et al. Grassland changes and adaptive management on the Qinghai–Tibetan Plateau. *Nat. Rev. Earth Environ.* **2022**, *3*, 668–683. [CrossRef]
9. Wang, Y.; Xue, K.; Hu, R.; Ding, B.; Zeng, H.; Li, R.; Xu, B.; Pang, Z.; Song, X.; Li, C.; et al. Vegetation structural shift tells environmental changes on the Tibetan Plateau over 40 years. *Sci. Bull.* **2023**, *68*, 1928–1937. [CrossRef]
10. Wei, Y.; Lu, H.; Wang, J.; Wang, X.; Sun, J. Dual Influence of Climate Change and Anthropogenic Activities on the Spatiotemporal Vegetation Dynamics Over the Qinghai-Tibetan Plateau From 1981 to 2015. *Earth's Future* **2022**, *10*, e2021EF002566. [CrossRef]
11. Yao, T.; Bolch, T.; Chen, D.; Gao, J.; Immerzeel, W.; Piao, S.; Su, F.; Thompson, L.; Wada, Y.; Wang, L.; et al. The imbalance of the Asian water tower. *Nat. Rev. Earth Environ.* **2022**, *3*, 618–632. [CrossRef]
12. Chen, J.; Chen, S.; Fu, R.; Li, D.; Jiang, H.; Wang, C.; Peng, Y.; Jia, K.; Hicks, B.J. Remote Sensing Big Data for Water Environment Monitoring: Current Status, Challenges, and Future Prospects. *Earth's Future* **2022**, *10*, e2021EF002289. [CrossRef]
13. Garbarino, M.; Morresi, D.; Anselmetto, N.; Weisberg, P.J. Treeline remote sensing: From tracking treeline shifts to multi-dimensional monitoring of ecotonal change. *Remote Sens. Ecol. Conserv.* **2023**, *9*, 729–742. [CrossRef]
14. Kamran, M.; Yamamoto, K. Evolution and use of remote sensing in ecological vulnerability assessment: A review. *Ecol. Indic.* **2023**, *148*, 110099. [CrossRef]
15. Kaplan, G.; Rashid, T.; Gasparovic, M.; Pietrelli, A.; Ferrara, V. Monitoring war-generated environmental security using remote sensing: A review. *Land Degrad. Dev.* **2022**, *33*, 1513–1526. [CrossRef]
16. Xu, H. A remote sensing urban ecological index and its application. *Acta Ecol. Sin.* **2013**, *33*, 7853–7862.
17. Li, Y.; Tian, H.; Zhang, J.; Lu, S.; Xie, Z.; Shen, W.; Zheng, Z.; Li, M.; Rong, P.; Qin, Y. Detection of spatiotemporal changes in ecological quality in the Chinese mainland: Trends and attributes. *Sci. Total Environ.* **2023**, *884*, 163791. [CrossRef]
18. Xiong, Y.; Xu, W.; Lu, N.; Huang, S.; Wu, C.; Wang, L.; Dai, F.; Kou, W. Assessment of spatial–temporal changes of ecological environment quality based on RSEI and GEE: A case study in Erhai Lake Basin, Yunnan province, China. *Ecol. Indic.* **2021**, *125*, 107518. [CrossRef]
19. Zhang, X.; Jia, W.; He, J. Spatial and temporal variation of ecological quality in northeastern China and analysis of influencing factors. *J. Clean. Prod.* **2023**, *423*, 138650. [CrossRef]
20. Manley, K.; Nyelele, C.; Egoh, B.N. A review of machine learning and big data applications in addressing ecosystem service research gaps. *Ecosyst. Serv.* **2022**, *57*, 101478. [CrossRef]
21. Meyer, H.; Pebesma, E. Machine learning-based global maps of ecological variables and the challenge of assessing them. *Nat. Commun.* **2022**, *13*, 2208. [CrossRef] [PubMed]

22. Stupariu, M.-S.; Cushman, S.A.; Pleşoianu, A.-I.; Pătru-Stupariu, I.; Fürst, C. Machine learning in landscape ecological analysis: A review of recent approaches. *Landsc. Ecol.* **2022**, *37*, 1227–1250. [CrossRef]
23. Liu, Q.; Qiao, J.; Li, M.; Huang, M. Spatiotemporal heterogeneity of ecosystem service interactions and their drivers at different spatial scales in the Yellow River Basin. *Sci. Total Environ.* **2024**, *908*, 168486. [CrossRef]
24. Qu, S.; Liu, J.; Li, B.; Zhao, L.; Li, X.; Zhang, Z.; Yuan, M.; Niu, Z.; Lin, A. Unveiling the driver behind China's greening trend: Urban vs. rural areas. *Environ. Res. Lett.* **2023**, *18*, 084027. [CrossRef]
25. Wang, Q.; Wang, X.; Zhou, Y.; Liu, D.; Wang, H. The dominant factors and influence of urban characteristics on land surface temperature using random forest algorithm. *Sustain. Cities Soc.* **2022**, *79*, 103722. [CrossRef]
26. Wang, Z.; Fu, B.; Wu, X.; Wang, S.; Li, Y.; Feng, Y.; Zhang, L.; Hu, Y.; Cheng, L.; Li, B. Distinguishing Trajectories and Drivers of Vegetated Ecosystems in China's Loess Plateau. *Earth's Future* **2024**, *12*, e2023EF003769. [CrossRef]
27. Minh, D.; Wang, H.X.; Li, Y.F.; Nguyen, T.N. Explainable artificial intelligence: A comprehensive review. *Artif. Intell. Rev.* **2022**, *55*, 3503–3568. [CrossRef]
28. Scott, M.; Su-In, L. A unified approach to interpreting model predictions. In Proceedings of the 31st International Conference on Neural Information Processing Systems, Long Beach, CA, USA, 4–9 December 2017; pp. 4768–4777.
29. Yao, L.; Han, Y.; Qi, X.; Huang, D.; Che, H.; Long, X.; Du, Y.; Meng, L.; Yao, X.; Zhang, L.; et al. Determination of major drive of ozone formation and improvement of O_3 prediction in typical North China Plain based on interpretable random forest model. *Sci. Total Environ.* **2024**, *934*, 173193. [CrossRef]
30. Yuan, Y.; Li, C.; Geng, X.; Yu, Z.; Fan, Z.; Wang, X. Natural-anthropogenic environment interactively causes the surface urban heat island intensity variations in global climate zones. *Environ. Int.* **2022**, *170*, 107574. [CrossRef]
31. Zhang, B.; Abu Salem, F.K.; Hayes, M.J.; Smith, K.H.; Tadesse, T.; Wardlow, B.D. Explainable machine learning for the prediction and assessment of complex drought impacts. *Sci. Total Environ.* **2023**, *898*, 165509. [CrossRef]
32. Office of the People's Government of Diqing Prefecture. Location and Area. Available online: http://www.diqing.gov.cn/dqgk/qwjmj.html (accessed on 15 August 2024).
33. Wang, W. The fundamental elements for maintaining social stability and their essential support. *People's Trib.* **2021**, 34–37. Available online: https://kns.cnki.net/kcms2/article/abstract?v=YK1b_MowDz-sfm27iXWpMKFUozbKH2aS3O48sEOMqmBxQlK91JgoDjTxWWZQHGp-ykogt-MzYJvXVXnVDUK4krC2DRSGf9fTkob4mJR5OQSjzSv9dEVrXo9tIzDcOWS8F0AqVTcyshqY2IPlcIaXXC-Hdv4MPaVQgNB-EpJdGsY66yzFzPF2GcFhS7IjGsIJ_4qujX6kqOE=&uniplatform=NZKPT&language=CHS (accessed on 11 September 2024).
34. Sen, P.K. Estimates of the regression coefficient based on Kendall's tau. *J. Am. Stat. Assoc.* **1968**, *63*, 1379–1389. [CrossRef]
35. Li, Y.; Li, Y.; Yang, X.; Feng, X.; Lv, S. Evaluation and driving force analysis of ecological quality in Central Yunnan Urban Agglomeration. *Ecol. Indic.* **2024**, *158*, 111598. [CrossRef]
36. Zhang, W.; Zhang, P.; Guo, S.; Lin, C.; Zheng, H.; Fu, P. Enhanced remote sensing ecological index and ecological environment evaluation in arid area. *Natl. Remote Sens. Bull.* **2023**, *27*, 299–317. [CrossRef]
37. Du, Z.; Ji, X.; Liu, J.; Zhao, W.; He, Z.; Jiang, J.; Yang, Q.; Zhao, L.; Gao, J. Ecological health assessment of Tibetan alpine grasslands in Gannan using remote sensed ecological indicators. *Geo-Spat. Inf. Sci.* **2024**, 1–9. [CrossRef]
38. Peng, S. *1-km Monthly Precipitation Dataset for China (1901–2023)*; National Tibetan Plateau/Third Pole Environment Data Center: Beijing, China, 2020. [CrossRef]
39. Running, S.; Mu, Q.; Zhao, M. *MODIS/Terra Net Evapotranspiration 8-Day L4 Global 500m SIN Grid V061*; NASA EOSDIS Land Process; DAAC: Sioux Falls, South Dakota, 2021. [CrossRef]
40. Shangguan, W.; Li, Q.; Shi, G. *A 1 km daily soil moisture dataset over China based on in-situ measurement (2000–2022)*; National Tibetan Plateau/Third Pole Environment Data Center: Beijing, China, 2022. [CrossRef]
41. Yan, K.; Yu, X.; Wang, J.; Myneni, R.B. *A High-Quality Reprocessed MODIS Fraction of Absorbed Photosynthetical ly Active Radiation Dataset (HiQ-FPAR)(Version 1)*; Zenodo: Genève, Switzerland, 2024. [CrossRef]
42. Zhang, H.; Luo, M.; Zhan, W.; Zhao, Y.; Yang, Y.; Ge, E.; Ning, G.; Cong, J. *A first 1 km High-Resolution Atmospheric Moisture Index Collection over China, 2003–2020*; National Tibetan Plateau/Third Pole Environment Data Center: Beijing, China, 2023. [CrossRef]
43. Buckley, S. *Nasadem Merged dem Global 1 arc Second v001 [Data Set]*; NASA EOSDIS Land Processes DAAC; USGS: Reston, VA, USA, 2020.
44. Xu, X. *The Spatial Distribution of China's GDP: Kilometer-Grid Dataset*; Resource and Environmental Science Data Platform: Beijing, China, 2017. [CrossRef]
45. Mu, H.; Li, X.; Wen, Y.; Huang, J.; Du, P.; Su, W.; Miao, S.; Geng, M. A global record of annual terrestrial Human Footprint dataset from 2000 to 2018. *Sci. Data* **2022**, *9*, 176. [CrossRef]
46. Prokhorenkova, L.; Gusev, G.; Vorobev, A.; Dorogush, A.V.; Gulin, A. CatBoost: Unbiased boosting with categorical features. In Proceedings of the 32nd International Conference on Neural Information Processing Systems, Montréal, QC, Canada, 2–8 December 2018; pp. 6639–6649.
47. Dorogush, A.V.; Ershov, V.; Gulin, A. CatBoost: Gradient boosting with categorical features support. *arXiv* **2018**, arXiv:1810.11363.
48. Zhao, Z.; Wu, X.; Li, G.; Li, J. Drought in southwestern China and its impact on the net primary productivity of vegetation from 2009–2011. *Acta Ecol. Sin.* **2015**, *35*, 350–360. [CrossRef]
49. Li, W.; Migliavacca, M.; Forkel, M.; Denissen, J.M.C.; Reichstein, M.; Yang, H.; Duveiller, G.; Weber, U.; Orth, R. Widespread increasing vegetation sensitivity to soil moisture. *Nat. Commun.* **2022**, *13*, 3959. [CrossRef]

50. Liu, Y.; Shan, F.; Yue, H.; Wang, X. Characteristics of drought propagation and effects of water resources on vegetation in the karst area of Southwest China. *Sci. Total Environ.* **2023**, *891*, 164663. [CrossRef]
51. Yao, Y.; Liu, Y.; Zhou, S.; Song, J.; Fu, B. Soil moisture determines the recovery time of ecosystems from drought. *Glob. Chang. Biol.* **2023**, *29*, 3562–3574. [CrossRef] [PubMed]
52. Zhu, Q.; Chen, H.; Peng, C.; Liu, J.; Piao, S.; He, J.-S.; Wang, S.; Zhao, X.; Zhang, J.; Fang, X. An early warning signal for grassland degradation on the Qinghai-Tibetan Plateau. *Nat. Commun.* **2023**, *14*, 6406. [CrossRef] [PubMed]
53. Yunnan Forestry and Grassland Bureau. Mutual Benefits between Ecological Protection and Economic Development in Diqing. Available online: https://lcj.yn.gov.cn/html/2021/meitikanlincao_0209/61397.html (accessed on 15 August 2024).
54. Ma, J. Daily Report on Building a New Socialist Modern Diqing: Ecological Protection Has Greened the Countryside and Beautified the Cities. Available online: http://www.xgll.com.cn/xwzx/2024-02/29/content_422167.htm (accessed on 15 August 2024).
55. Zhao, Z.; Dai, E. Vegetation cover dynamics and its constraint effect on ecosystem services on the Qinghai-Tibet Plateau under ecological restoration projects. *J. Environ. Manag.* **2024**, *356*, 120535. [CrossRef] [PubMed]
56. General Office of the People's Government of Yunnan Province. Notice from the People's Government of Yunnan Province on the Publication of the Ecological Protection Red Line in Yunnan Province (No. 32 [2018]). Available online: https://www.yn.gov.cn/zwgk/zcwj/zxwj/201911/t20191101_184159.html (accessed on 15 August 2024).
57. Hu, P.; Zhou, Y.; Zhou, J.; Wang, G.; Zhu, G. Uncovering the willingness to pay for ecological red lines protection: Evidence from China. *Ecol. Indic.* **2022**, *134*, 108458. [CrossRef]
58. Zhang, Y.; Guan, D.; Wu, L.; Su, X.; Zhou, L.; Peng, G. How can an ecological compensation threshold be determined? A discriminant model integrating the minimum data approach and the most appropriate land use scenarios. *Sci. Total Environ.* **2022**, *852*, 158377. [CrossRef]
59. Du, Q. Study on the Ecological Compensation of "Three Parallel Rivers" Region of Western Yunnan. *J. Yunnan Adm. Coll.* **2017**, *19*, 151–157. [CrossRef]
60. Zhang, Q.; Yuan, R.; Singh, V.P.; Xu, C.-Y.; Fan, K.; Shen, Z.; Wang, G.; Zhao, J. Dynamic vulnerability of ecological systems to climate changes across the Qinghai-Tibet Plateau, China. *Ecol. Indic.* **2022**, *134*, 108483. [CrossRef]
61. Tilman, D.; Downing, J.A. Biodiversity and stability in grasslands. *Nature* **1994**, *367*, 363–365. [CrossRef]
62. MacGillivray, C.; Grime, J.; The Integrated Screening Programme (ISP) Team. Testing predictions of the resistance and resilience of vegetation subjected to extreme events. *Funct. Ecol.* **1995**, *9*, 640–649. [CrossRef]
63. Yu, Q.; Lu, H.; Yao, T.; Xue, Y.; Feng, W. Enhancing sustainability of vegetation ecosystems through ecological engineering: A case study in the Qinghai-Tibet Plateau. *J. Environ. Manag.* **2023**, *325*, 116576. [CrossRef]
64. Chen, N.; Zhang, Y.; Zu, J.; Zhu, J.; Zhang, T.; Huang, K.; Cong, N.; Wang, Z.; Li, J.; Zheng, Z. The compensation effects of post-drought regrowth on earlier drought loss across the tibetan plateau grasslands. *Agric. For. Meteorol.* **2020**, *281*, 107822. [CrossRef]
65. Lu, L.; Shen, X.; Cao, R. Elevational movement of vegetation greenness on the Tibetan Plateau: Evidence from the Landsat Satellite Observations during the Last Three Decades. *Atmosphere* **2021**, *12*, 161. [CrossRef]
66. Zhang, L.; Shen, M.; Yang, Z.; Wang, Y.; Chen, J. Spatial variations in the difference in elevational shifts between greenness and temperature isolines across the Tibetan Plateau grasslands under warming. *Sci. Total Environ.* **2024**, *906*, 167715. [CrossRef] [PubMed]
67. Lai, J.; Zhao, T.; Qi, S. Spatiotemporal Variation in Vegetation and Its Driving Mechanisms in the Southwest Alpine Canyon Area of China. *Forests* **2023**, *14*, 2357. [CrossRef]
68. Gao, B.; Wu, Y.; Li, C.; Zheng, K.; Wu, Y.; Wang, M.; Fan, X.; Ou, S. Multi-scenario prediction of landscape ecological risk in the Sichuan-Yunnan ecological barrier based on terrain gradients. *Land* **2022**, *11*, 2079. [CrossRef]

Disclaimer/Publisher's Note: The statements, opinions and data contained in all publications are solely those of the individual author(s) and contributor(s) and not of MDPI and/or the editor(s). MDPI and/or the editor(s) disclaim responsibility for any injury to people or property resulting from any ideas, methods, instructions or products referred to in the content.